Advances in Science and Technology Research Journal

Advances in Science and Technology Research Journal, 18(7), 1–17
https://doi.org/10.12913/22998624/191077
ISSN 2299-8624, License CC-BY 4.0

Received: 2024.05.20
Accepted: 2024.08.15
Published: 2024.10.06

Design of a Lever Hydroelectric Power Plant – in the Structural Aspect with a Strength Analysis of the Selected Segment

Paweł Gwizdal[1*], Arkadiusz Gola[1]

[1] Department of Informatization and Robotization of Production, Lublin University of Technology, ul. Nadbystrzycka 36, Lublin, Poland

* Corresponding author's e-mail: p.gwizdal@pollub.pl

ABSTRACT

This article presents examples of the use of complex sheet metal in everyday life and the course of modeling a sheet bent simultaneously in two planes. The element selected to describe the modelling process is a fragment of the side wall of a lever hydroelectric power plant that operates on the Bystrzyca River in Lublin. The shape of the element is conditioned by the need to achieve a gentle change in the cross-section of the water stream during the flow between the steering system and the outflow area. The segment through which the water flows is clearly lower and wider than the other modules of the power plant, which is due to the average water level in the Bystrzyca River. Such a shape is necessary because the inflow and outflow parts of the power plant must be submerged under water all the time. This is due to the principle of operation of the power plant, which works by obtaining a vacuum created by pumping air from the inside. The article also presents the results of the strength analysis, which was performed for the segment exposed to the highest loads. The analysis and the entire design were performed in Autodesk Inventor, and the results obtained were as expected and even in the most critical places no values were reached that would require changes to the design.

Keywords: modeling, inventor, bent plate, hydroelectric power plant, FEM.

INTRODUCTION

Sheet metal elements made of various types of steel are currently widely used in many industries. This is due to a number of advantages, among which the most important are:

- High strength,
- Easy to form,
- Ability to create complex, three-dimensional shapes,
- Favorable steel price [1].

The ability to obtain complex, unusual shapes, while maintaining high strength, are the decisive factors for the use of sheet metal elements in many different constructions. The most important areas include:

1. Automotive – first of all, the production of car bodies and vehicle interior elements, where a very important requirement is to obtain the right shape, with the lowest possible weight and high strength. In recent years, the development of hybrid and electric cars has been noticeable, which is associated with an increase in the requirements for car bodies [2]. Despite this, the material from which they are made does not change, which proves the huge potential of sheet metal elements in terms of modification and shaping. The importance of the ability to obtain complex shapes for the automotive industry is perfectly demonstrated by the illustration above (Figure 1), where the color of sheet metal elements is highlighted. As you can see, almost the entire supporting structure is made of various types of steel, and many elements are characterized by a complex shape [2].
2. Aerospace – where sheet metal components play a very important role in the construction

Figure 1. Chrysler car support structure [3]

of the fuselage, wings, skin and interior of the aircraft. The ability to produce thin-walled components with complex shapes, and thus the lightest possible ones that do not lose strength, is a key requirement in the entire aerospace industry [4, 5]. In order to illustrate the importance of sheet metal elements in the construction of an aircraft, Figure 2 is attached, showing the skeleton of an exemplary sports aircraft – ZODIAC. Its entire load-bearing structure consists of 342 bent or flat sheets (flat parts should be understood as elements that have not been bent, but only the desired shape has been cut out – mainly ribbing) [6].

3. Marine – in which sheet metal is used to make elements of ships, sometimes of a very complex shape. A fundamental requirement in this industry is to obtain a fully sealed structure with a buoyancy greater than the maximum weight provided. In ship building, bent plate can be used for the following assemblies:

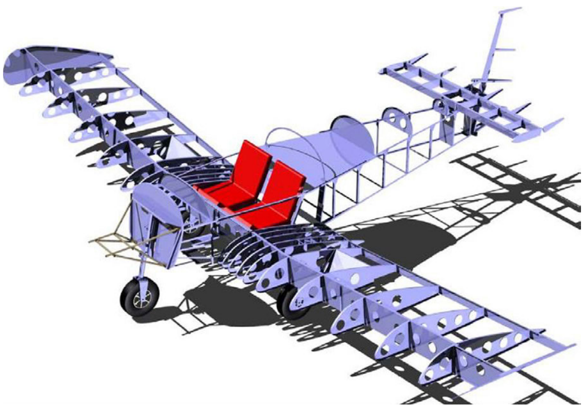

Figure 2. 3D model of the ZODIAC aircraft frame structure

- hull,
- deck,
- mast - it's design usually depends on the structure of the hull,
- cargo warehouses and passenger and crew cabins [7, 8].

4. Architecture and construction – where there are plenty of examples of the use of sheet metal. The most well-known structure in this area is the tin garage, but there are also other:
   - roofs and façade elements of buildings (often very complex in shape)),
   - tank plating,
   - bridge construction elements.

   In the construction industry, sheet metal elements have now become a very important link in many structures. This is closely related to the development of CAD (computer aided design) programs that allow you to control the shape of the object at every stage of design, which leads to the maximum use of the potential of sheet metal and the creativity of the architect [9].
5. Railway industry – which is very demanding in terms of the durability of the solutions used. In this industry, almost entire wagons are sometimes made of bent sheets, an example of which is shown in Figure 3. The use of bent sheet metal is not limited to train/subway construction. This solution is an inseparable component of railway equipment covers, track infrastructure and platform roofing.
6. Mining – an industry in which you can give a whole lot of examples of the use of bent sheet metal with varying degrees of shape complexity. Here are a few of them:

Figure 3. Siemens Inspiro electric subway car (left) and its sheet metal support structure (right) [10]

- pneumatic conveying systems – used wherever there is a risk of explosion, which makes it very limited or impossible to use systems driven by electric motors [11],
- skip – a device used to bring to the surface raw materials obtained by miners [12],
- lining the walls of mine shafts – a fundamental requirement for safety when working in mines. The side walls of the shaft are protected against subsidence in order to minimize the risk of collapse. For this purpose, various solutions are used, e.g. a properly formed steel sheet is laid on a leveled wall, reinforcement is placed and shotcrete is poured, and the whole is supported by a reinforced concrete column [13],
- conveyors [14] – commonly used in the mining industry, due to their high efficiency, low operating costs, high versatility and reliability, and low environmental impact compared to other means of material handling [15].

7. Robots and robotic equipment – without which it is hard to imagine the functioning of many industries today. Structural elements such as chassis of mobile robots, load-bearing structure, arms of industrial robots, or housing are very often made of bent sheet metal, which gives the possibility of obtaining the desired shape, optimal weight and required strength (Figure 4) [16, 17, 18, 19]. Sheet metal is also often used to make robot effectors, i.e. the ends of the arms that allow it to interact with the environment (grasping an object, measuring, painting, etc.) [20].
8. Construction and agricultural machinery – for which the requirements in terms of permissible loads, rigidity, durability, reliability, ergonomics and maximum weight reduction are constantly increasing, while maintaining the highest safety standards [21, 22]. Sheet metal components are commonly used to provide optimal solutions, taking into account the above aspects. Both of these industries also have countless examples of the use of bent sheet metal, often having a complex shape. Construction machinery with sheet metal elements is m.in excavators, bulldozers, wheel loaders and cranes. In agriculture, they can be found, for example, in the construction of semi-trailers, chopping machines, soil processing machines, agricultural processing equipment, tractors or livestock buildings. This article aims to present the effects of work on the project of a small hydroelectric power plant (lever power plant), which has been operating on the Bystrzyca River in Lublin for nearly three years. The main aspect on which the focus is the construction aspect and strength tests. The project was

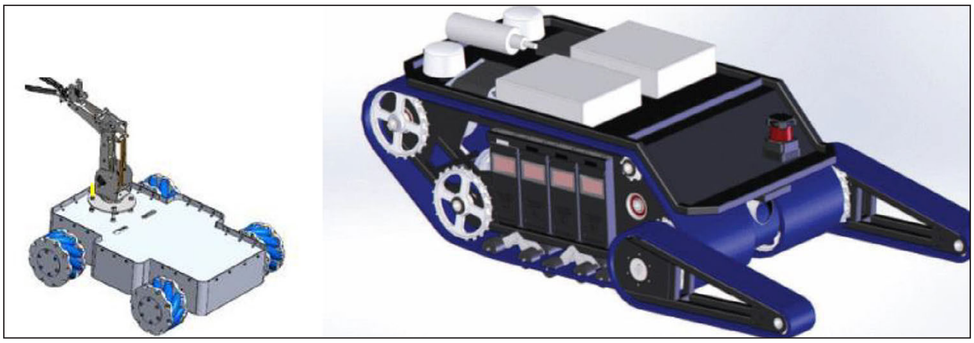

Figure 4. Construction of a small mobile transport robot (left) [16] and a large platform robot (right) [17]

made using Autodesk Inventor Professional 2016 software. Strength calculations were also carried out in this program, using the stress analysis module, which is based on finite elements (in this case, the analyzed structure is divided into pyramids).

The second objective of the article is to promote the use of renewable sources of electricity in Poland, with an emphasis on solutions belonging to hydropower, the potential of which in this country is unfortunately small. The lack of natural water thresholds with a significant difference in water levels makes it impossible to build large dams, and the low tidal phenomenon in the Baltic Sea makes it very difficult to build tidal power plants here. That is why small hydroelectric power plants in Poland are very promising in the context of hydropower.

HYDROPOWER IN POLAND

Watercourse energy is one of the most promising renewable sources of electricity. A number of advantages of this source have resulted in the fact that there are many different types of hydroelectric power plants operating all over the world, which are adapted to the terrain and climatic conditions of a given region. The electricity obtained in this way is referred to as „clean energy" because there is no emission of substances harmful to the atmosphere and there is no waste in the process of converting the potential energy of water.

In Poland, due to the amount of precipitation, the relief of the terrain and the low tidal phenomenon of the Baltic Sea, there are no conditions for the construction of hydroelectric power plants on a large scale. You can't change the environment, so you have to adapt to it, and that's where small hydroelectric power plants come in. They are based on existing water thresholds, which occur in Poland on many rivers, e.g. as remnants of mills. In such places, it is easy to obtain a building permit, which attracts potential investors [23]. According to various sources, there may be between 700 and 1000 installations of this type in Poland at the turn of 2023 and 2024.

The element selected to present the modelling process comes from the construction of a lever hydroelectric power plant (Figure 5), which was implemented on the Bystrzyca River in Lublin in June 2021.

The operation of the lever system is based on the phenomenon of gravity combined with the pressure of water. The inflow is positioned 700 mm higher than the outflow, thus forcing the direction of liquid flow. The water is compressed as it approaches the rotor, which accelerates, and its energy is maximally utilized when it is transferred to the generator rotor (Figure 6).

In order to increase the rotational speed on the generator, a belt transmission with a ratio of 1:4.5 was used. This solution made it possible to use a commercial generator with a nominal rotational speed of 740 rpm, with a nominal power of 30 kW.

ANALYSIS OF THE SIDE WALLS OF THE DISCHARGE PART

The most difficult stage of modelling was the execution of the side walls of the outflow part, which consists of the last three segments (on the left side in Figure 5). One of these plates is shown in Figure 7.

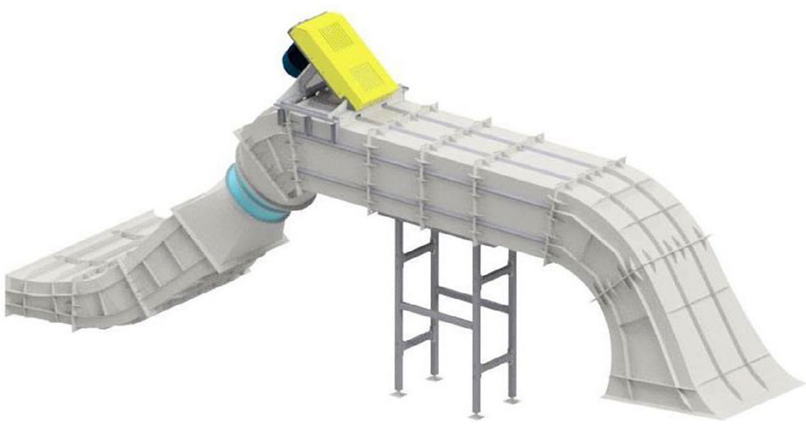

Figure 5. 3D model of a lever hydroelectric power plant [23]

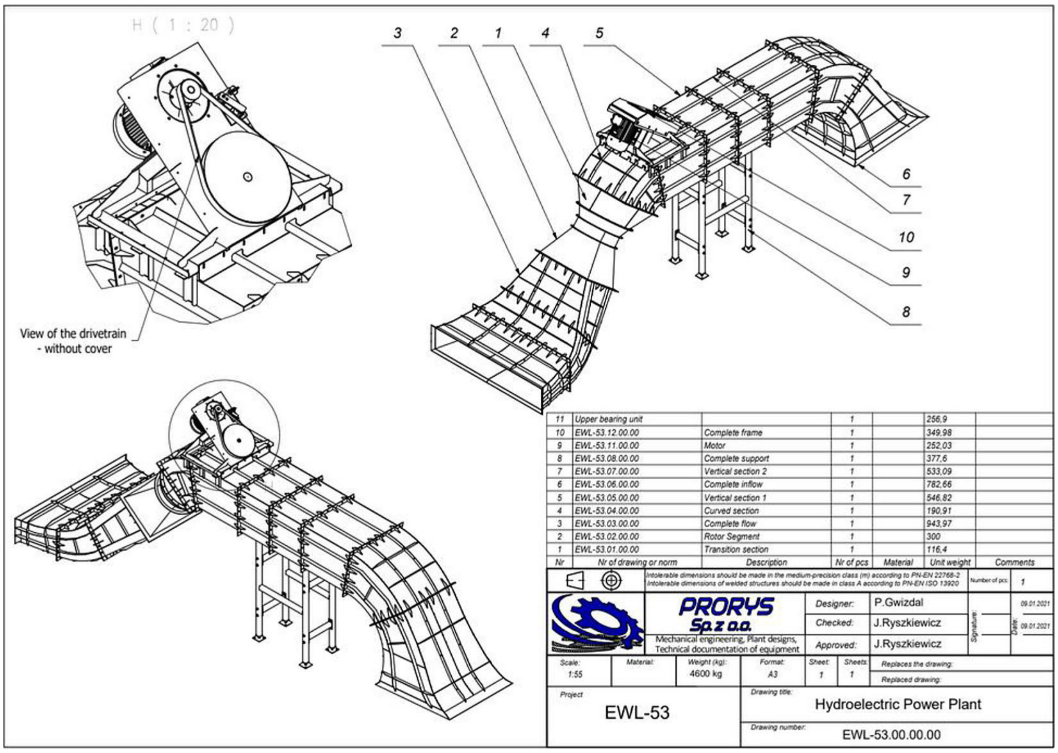

Figure 6. Presentation of the drivetrain without a cover

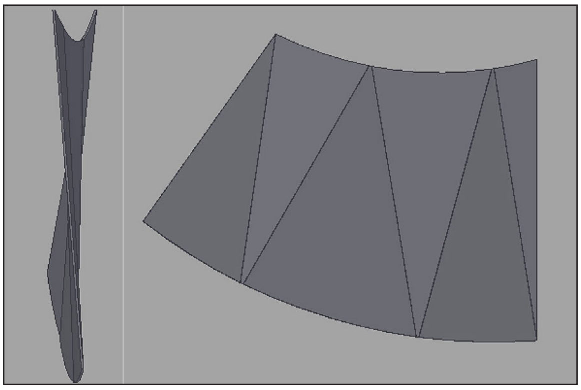

Figure 7. Isolated side wall of one of the outflow segments, front view (left), side view (right)

The shape of the element is determined by several aspects. Firstly, the power plant was designed taking into account the profile of the riverbed and the existing water threshold, which is a remnant of another power plant. The second factor influencing the shape is that the change in the cross-section of the water stream must be gentle, so that there is no splashing of water as it flows through the subsequent segments. The third aspect concerns the way in which the power plant operates. The inflow and outflow must be below the water table at all times, as the system operates on the principle of vacuum, which means that no air can enter the system. As a result, the outflow area is the lowest and widest part of the power plant, and its side walls made of sheet metal are characterized by a very non-standard geometry. Modeling of one of these plates (Figure 7) will be presented later in this article.

MODELLING

The development of CAD programs has provided the construction industry with many very useful tools to improve work at every stage of the project, from the initial idea, through the implementation of models in terms of execution, to simulations and drawing documentation. The possibility of three-dimensional visualization of the designer's ideas means that solution concepts can be presented to the customer in the form of a simplified solid model, so that he can indicate his comments or choose the optimal solution for himself if an idea has appeared. After making the necessary corrections and approval from the client, you can proceed to the implementation of the project. At this stage, the simplified model used for visualization is mapped in the form of assemblies consisting of elements that can be physically made and connected to each other. When the work on the 3D (3 dimension) model is completed, a strength analysis can be performed, and if it gives a result that meets the safety requirements, the design part is completed. The last stage is to simulate the functioning of the designed solution and prepare drawing documentation, which is sent to the people involved in the production of the required elements and assembly.

The project of the lever hydroelectric power plant was implemented in accordance with the above course. The whole is divided into segments/modules to ensure trouble-free transport to the power plant site and quick and easy installation. The individual segments were screwed together with M16 screws, sealing the contact area with felt to ensure one hundred percent tightness. Apart from the supporting structure, flanges and ribs, all components of the power plant are made of bent sheet metal.

The vast majority of work on the model did not require complex geometry. The exception was the side walls of the outflow segments. The modeling step of these elements was carried out in the context of the assembly, and it was as follows:

Setting of reference elements – in the form of flanges connecting individual components of the power plant. The setting was made on the basis of the initial model, accepted by the investor.

Making a sketch – fully bound with as few dimensions as possible. All sketches in this type of project should be made in such a way that they can be easily edited, which allows you to use them later and save time by not remodeling two elements with similar geometry. Some dimensions can be replaced by relations that, regardless of dimensional corrections, will ensure the constancy of a specific feature (such as perpendicularity, parallelism, collinearity). In this step, the shape and dimensions were adapted to the end flanges of the segment, shown in

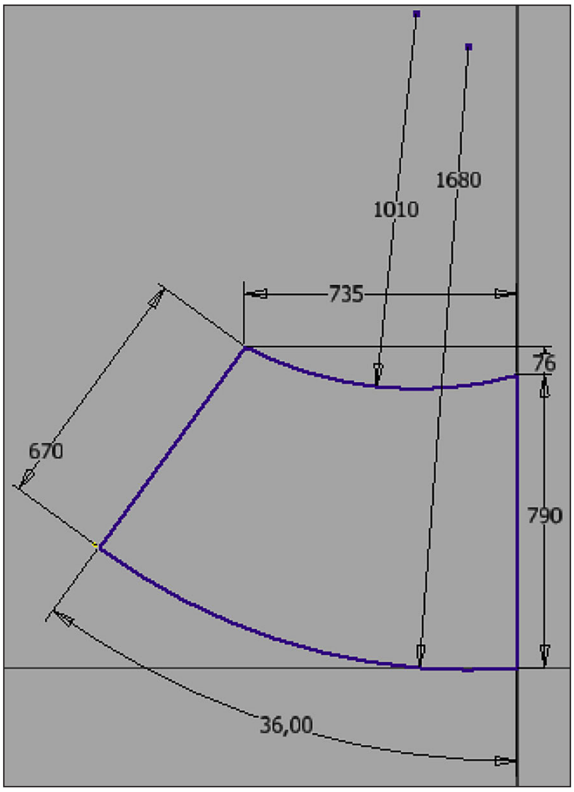

Figure 9. Sketch of the modeled sidewall

Figure 8, 9. Defining the thickness of the element – 4 mm. All sheet metal elements have the same thickness, except for the flanges connecting the segments, which are made of 8 mm thick flat bar (Figure 10).

First wrap – sketch and execution. All bending operations were performed using the „Wrap" tool. To do this, a bending line had to be defined. At the modeling stage, it was noticed that the best effect would be achieved by inclination of the flange in relation to the edge welded to the flange. The change in the shape of the segment turned out to be smoother than in the case of bending along a line parallel to the reference Edge (Figure 11).

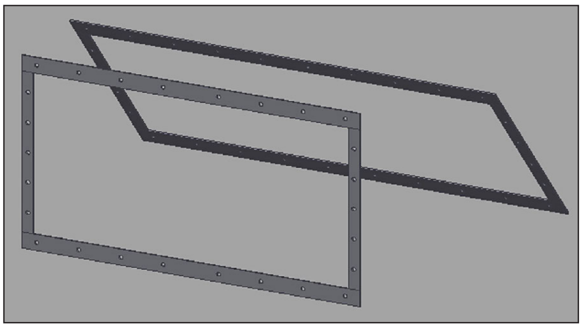

Figure 8. Flanges of the middle segment of the flow part – a pattern for modeling the side walls

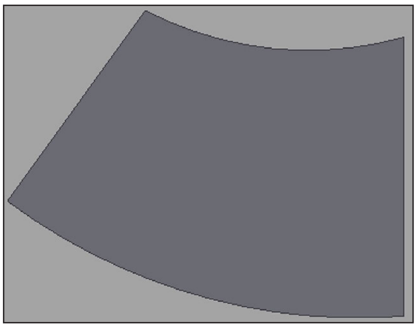

Figure 10. View of the element after defining the thickness

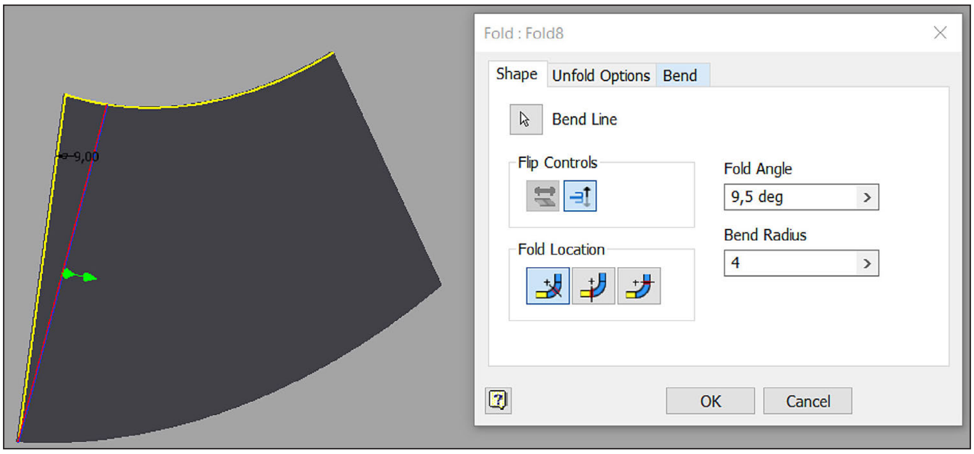

Figure 11. Sketch and first fold dialog pro

Second wrap – initially made at the same angle as the first. However, in such elements it is very difficult to achieve a perfect fit with other components and in the end, it was necessary to slightly correct some of the bending angles (Figure 12). Third fold – the middle one, with a bend angle of 10°, which was also determined at the stage of fitting to the end flange (Figure 13).

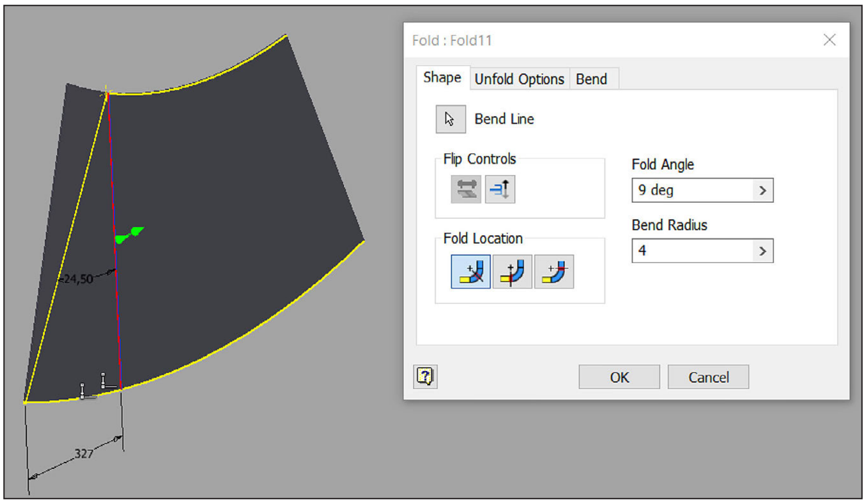

Figure 12. Sketch and second fold dialog

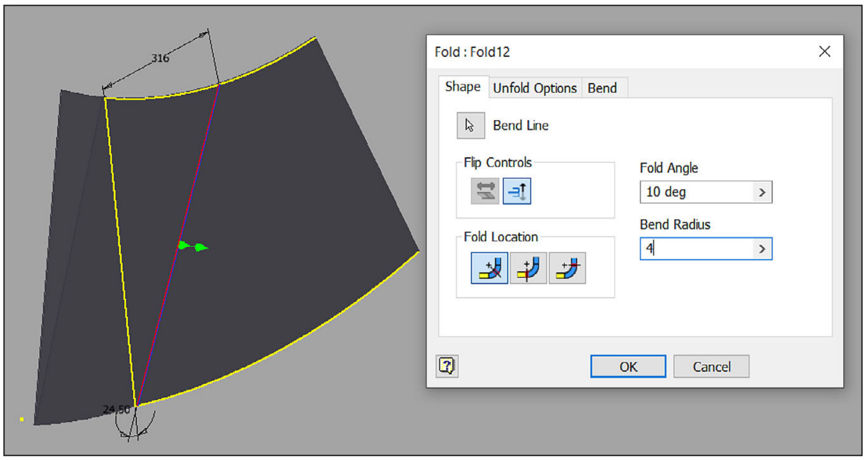

Figure 13. Sketch and third fold dialog the fourth fold – the penultimate one with a fold angle of 8°.

Fifth fold – the last one, after which the final shape of the element was obtained. In the end, all calls were in the range of 8–10. Despite the fact that this was the last operation, it was still necessary to introduce an element to assemble the power plant section (Figure 14, 15). Bending angle compensation – to match the sidewall to both flanges. The assembly was made by placing one edge welded in the flange with a tangent relation. The welded edge with the second flange had to be adjusted by correcting the wrap angles (Figure 16). Making the second side wall – with the help of a mirror image. The entire structure (except for the drive system) has a plane of symmetry. Therefore, some of the elements could be made as a mirror image of previously modeled components (Figure 17). The

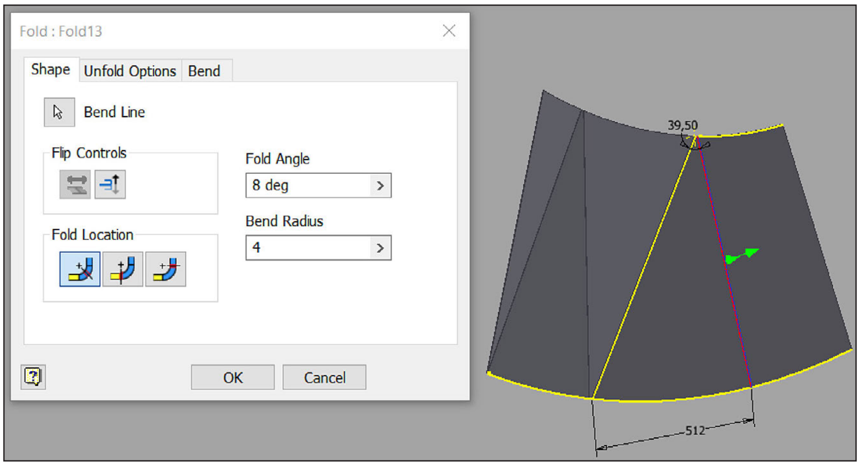

Figure 14. Sketch and fourth wrap dialog

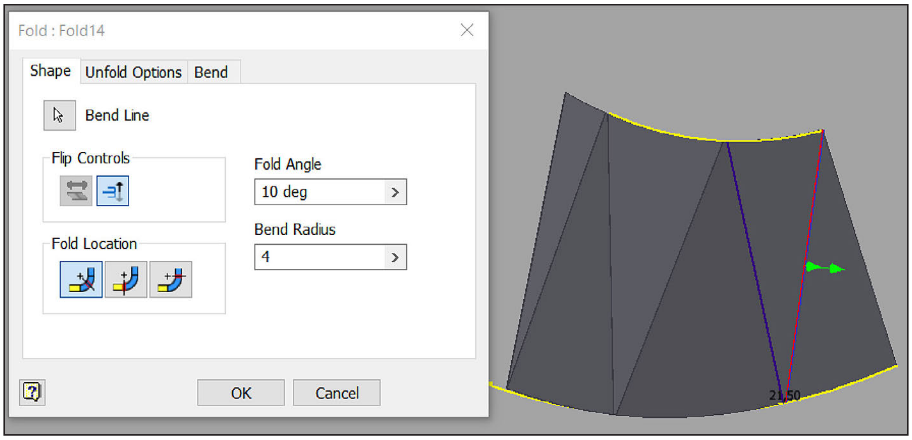

Figure 15. Sketch and fifth wrap dialog

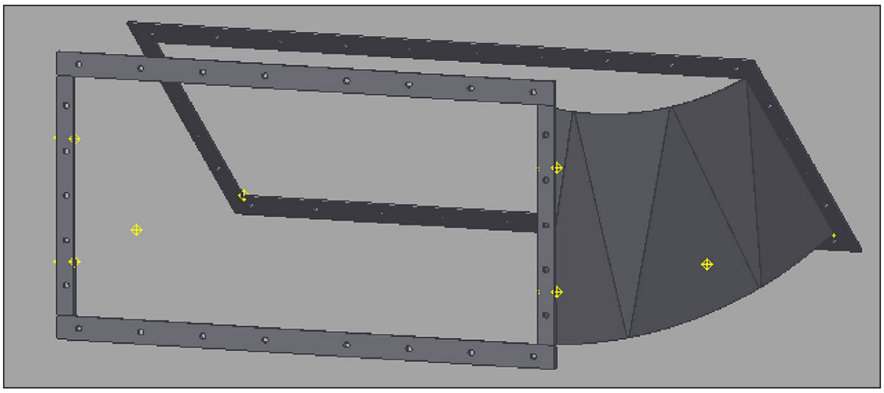

Figure 16. Sidewall inserted into the flanges connecting the segments

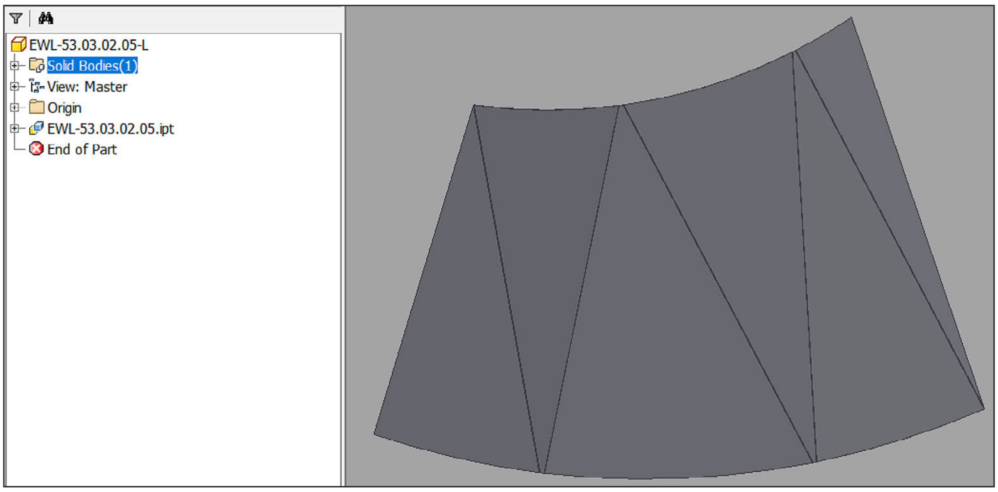

Figure 17. Segment sidewall made as mirror image

geometry of the reflected element adapts to the source element and changes if it is modified.

PRESENTATION OF THE ELEMENT IN THE CONTEXT OF THE ENTIRE SEGMENT

The final model of the segment is shown in Figure 18. The model in Figure 18 is an entirely welded assembly. Apart from the side walls, the ribbing and the lower and upper walls are characterized by complex geometry. However, these elements did not require an unconventional modelling approach, but also had to be designed in the context of the assembly. The designer's working time on the side wall was 1 hour, which is exactly the same as on the assembly and all other elements of the entire member. This perfectly illustrates the level of difficulty he had to face during the modeling process.

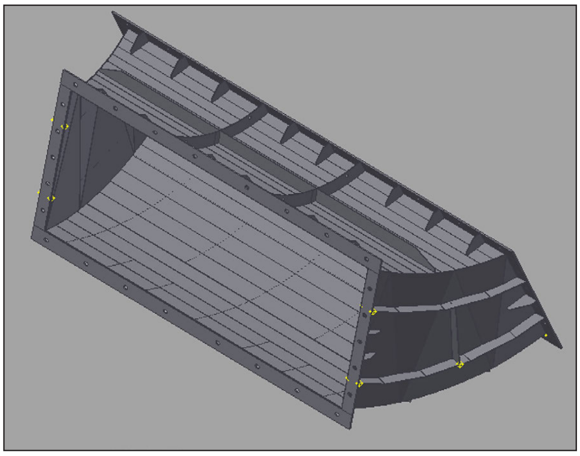

Figure 18. Middle segment of the outflow part

FEM (FINITE ELEMENT METHOD) STRENGTH ANALYSIS

The last and most important stage of the project was to carry out a strength analysis of the most stressed segment of the power plant.

Determination of the forces acting on the power plant - analysis of boundary conditions

At the design stage, the forces acting on each segment were calculated. The most heavily loaded module of the power plant turned out to be the arc module, marked in blue in Figure 19. The forces acting on this segment come from the mass of the flowing water (in the outflow part), the pressure of the water in the narrowing area, the mass of the structure suspended under the segment and the mass of the element itself (the force of gravity). Other factors affecting the power plant were found to be negligible compared to the forces mentioned, which can therefore be considered as the only existing boundary conditions. At this point, it is also worth mentioning how the threats resulting from the presence of fish and birds that could get inside the installation were dealt with. Well, it has been tightly secured with a WEMA grille, which prevents fish, birds or dirt from getting inside that could interfere with the operation of the power plant. The mode of operation of these forces is defined in the program and graphically shown in Figure 20. Calculation of the forces acting on the most loaded part of the power plant:

- Thrust force of the liquid – marked in yellow. It acts on the top wall and is derived

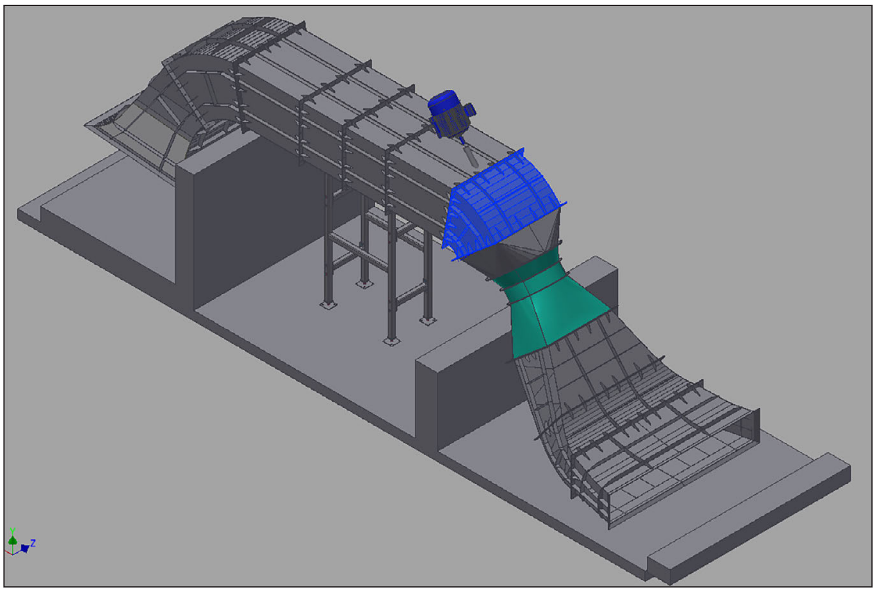

Figure 19. Presentation of the busiest segment of power plants

Table 1. Calculation of the force due to the pressure of a liquid

Parameter	Value	Unit
ρ	997	kg/m^3
A	1.54	m^2
c	1.5	–
V	2.5	m/s
F	7197	N

from the velocity of the water and its cross-section in the segment area. The dynamic thrust equation (formula 1) was used to calculate this force, and the results of the calculation are presented in the Table 1.

$$F = \frac{1}{2} \cdot \rho \cdot A \cdot c \cdot V^2 \text{ [N]} \tag{1}$$

where: ρ – water density [kg/m^3], A – Segment cross-section [m^2], c – dynamic drag coefficient – assumed for the most unfavorable case (the highest value among the range found in the literature items), V – water flow velocity [m/s].

The force coming from the mass of the water in the segment area and the water pressure in the choke area is shown in blue. It acts on the bottom wall and flange and comes mainly from the volume of water in the segment area (calculated from formula 2). The constriction component was calculated from the thrust formula (4), using the Venturi equation to determine the pressure difference (3). The results of the calculations are presented in Tables 2, 3 and 4.

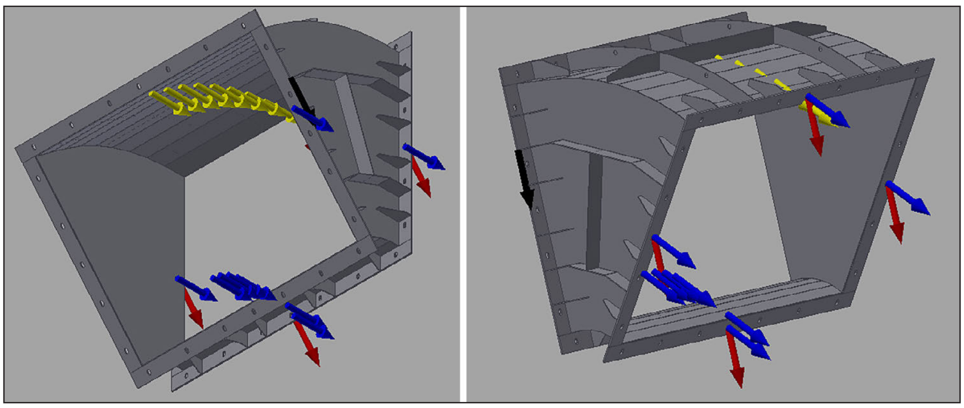

Figure 20. Graphical representation of the forces acting on the analyzed segment

Table 2. Calculation of the force coming from the mass of water in the segment

Parameter	Value	Unit
m	1080	kg
g	9.81	m/s^2
F	10595	N

Table 3. Calculation of the force due to the pressure of the liquid in the constriction region

Parameter	Value	Unit
ρ	997	kg/m^3
A1	2.54	m^2
A2	0,75	m^2
V	2.5	m/s
P1-P2	2180	Pa

Table 4. Calculation of the force coming from constriction

Parameter	Value	Unit
P1-P2	2180	Pa
A2	0.75	m^2
F	1643.5	N

- Calculations of the component derived from the mass of water

$$F = m \cdot g \text{ [N]} \tag{2}$$

where: m – mass of water inside the segment [kg], g – acceleration due to gravity [m/s^2].

- Calculations of the component derived from the constriction

$$P1 - P2 = \frac{1}{2} \cdot \rho \cdot V^2 \left(1 - \frac{A2}{A1}\right) \text{ [N]} \tag{3}$$

where: $P1$ – pressure before constriction [Pa], $P2$ – pressure at the exit from the throat area [Pa], ρ– water density [kg/m^3], V – water flow velocity [m/s], $A1$ – cross-sectional area of water stream before constriction [m^2], $A2$ – cross-sectional area of the water stream at the exit of the constriction area [m^2].

Calculation of the thrust force due to the constriction

$$F = (P1 - P2) \cdot A2 \text{ [N]} \tag{4}$$

where: $P1$–$P2$ – pressure difference calculated by the Venturi equation [Pa], $A2$ – cross-sectional area of the water stream at the exit of the constriction area [m^2].

After adding up the two calculated components, a force of 12 238.5 N. The force from the weight of the flow part and the steering system is shown in red. This force consists of the steering mass (highlighted in green in Figure 19), the mass of the transition module (between the green and blue segments in Figure 19) and the mass of the discharge. The factors influencing this force should also include the mass of the liquid above the water table, in the part of the power plant suspended on the analyzed segment. The calculations were made on the basis of formula 2. The results of the calculations are presented in the Tables 5 and 6.

The volume of liquid above the water table in the analyzed part of the power plant is 2.69 m^3. The mass of water used for calculations (parameter m, Table 6) is the product of its volume and its own weight. The final value of the third force acting on the analyzed segment is the sum of both calculated components: 12 360.6 N + 26 310 N = 38 670.6 N.

Course of the FEM analysis

After defining the forces acting on the power plant, performing the necessary calculations and determining the member on which the greatest forces act, the FEM calculations began. A fixed constraint is defined on the flange surface by means of which the analyzed segment is bolted to the preceding horizontal member. The grid was also plotted and its parameters defined, achieving the effect shown in Figure 21.

During the analysis, the key parameters are the Von Mises stresses, the magnitude of

Table 5. Calculation of the force coming from the mass of suspended segments

Parameter	Value	Unit
m	1260	kg
g	9.81	m/s^2
F	12 360.6	N

Table 6. Calculations of the force coming from the mass of the liquid above the water table in suspended members

Parameter	Value	Unit
ρ	997	kg/m^3
m	2682	kg
g	9.81	m/s^2
F	26 310	N

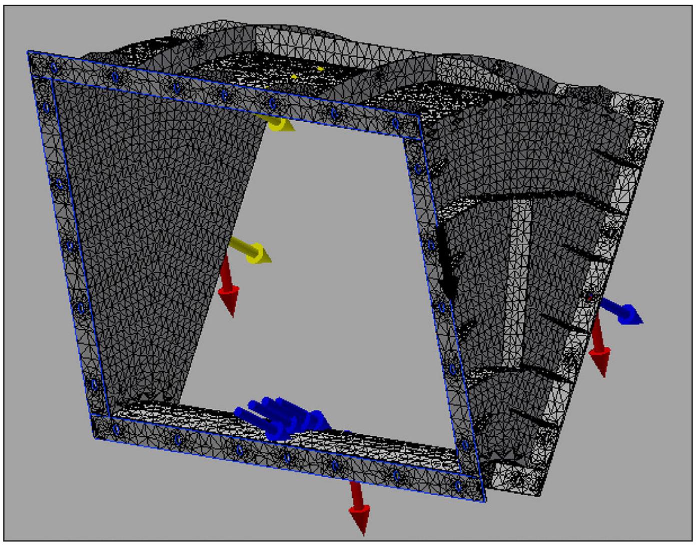

Figure 21. Meshed segment prepared for FEM analysis

displacements, and the factor of safety. The calculations were performed in the stress analysis module of Autodesk Inventor Professional 2016. The description of the solid model was carried out using TETRA elements, which is the only type that is in Inventor. The analyzed area was divided into pyramids, so that there are at least two finite elements on the thickness of each element.

Von mises stress analysis

The results of Von Mises' analysis are presented in Figure 22. The maximum stresses that occurred are 193.4 MPa, which is lower than the allowable stresses of 225 MPa – the value for the S235JR steel, from which the entire power plant is made. In Figure 22, the display of results has been modified. The upper threshold for color-coding stress locations has been reduced from 193.4 MPa to 120 MPa. This procedure was performed due to the point nature of the stresses, which appear only in the ribs of the lower wall and at the flange on which the steering section and the outflow part of the power plant are suspended. With the initial display settings, the stress area was not visible. The greatest stresses occur at the point of contact between the edge of the top panel and the flange and the side wall, i.e. at the point of contact between the four sheets. A weld has been

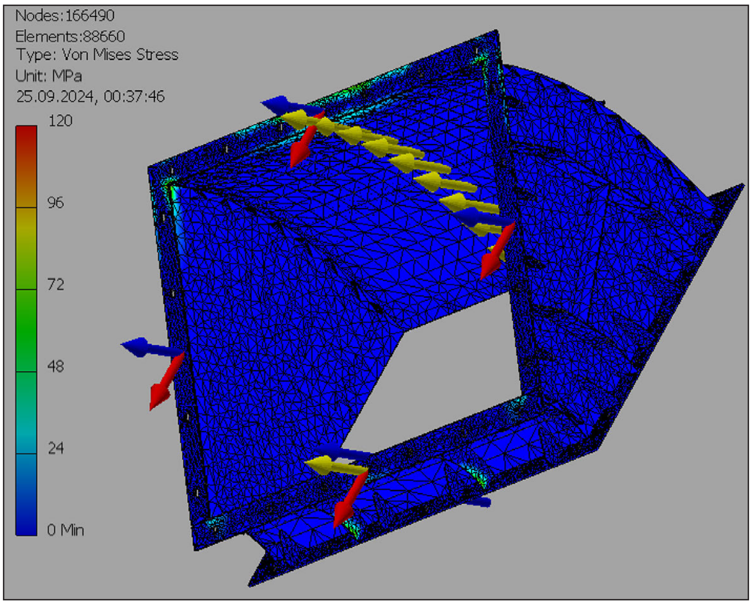

Figure 22. FEM calculation results – Von Mises stresses

laid in these corners during assembly, and another member is screwed to the flange, so the actual stress values will be lower than 193.4 MPa.

Displacement analysis

The results of the displacement analysis are shown graphically in Figure 23. According to calculations, the maximum deformation will be 1.7 mm, which is the permissible value in this type of construction. The place where the greatest displacements occur is the upper part of the flange, to which the segments of the flow part and the member with the steering system are attached. In addition to the flange, the upper wall near the connection with the next segment is deformed. However, these displacements are much smaller and oscillate around 1 mm. It should be noted that the calculated values will actually be smaller. In the place of the maximum deformations, the flange of the next power plant member is screwed, which will distribute the load over the entire flange, and finally reduce the actual deformations in relation to the calculated value.

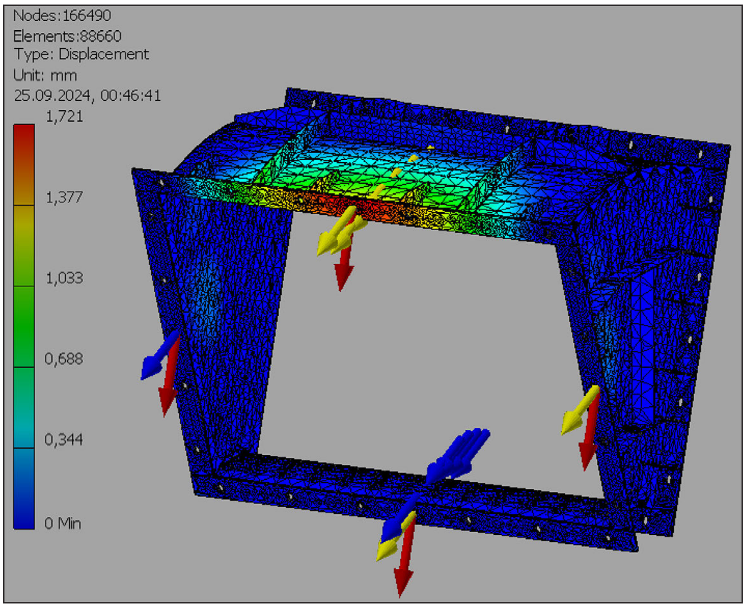

Figure 23. Displacement analysis results

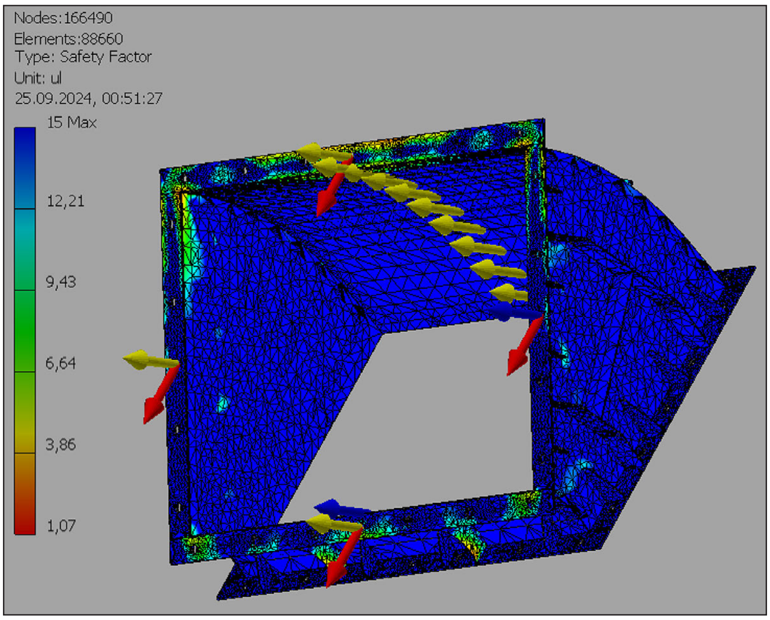

Figure 24. Results of the analysis in terms of the obtained safety factor

Factor of safety

The results of the FEM analysis in terms of the obtained safety factor are presented in Figure 24. The smallest value that appears is 1.07 and occurs near the area where the greatest stress occurred. A value of 1.07 means that the strength of the material is slightly higher than the assumed loads, but due to the point occurrence and location at the junction of four sheets, this value is safe and fully acceptable. It is important to note that the coefficient at this point will actually be greater because it is the place where the weld was placed during the installation process.

It should be noted that Figure 24 distinguishes small areas within the flange to which the force has been applied and on the bottom reinforcement (in the ribs). In these places, the value of the coefficient oscillates between 3 and 6, so it is a very safe value.

Accuracy of calculations

The most important criterion that was crucial in the entire analysis was the Von Mises stresses. The first calculations, the results of which are presented in Figures 22–24, were carried out for the minimum acceptable mesh density (i.e. the one where there are at least 2 finite elements on the thickness of the element). Then, for more accurate results, the mesh density was increased from 0.1 to 0.5 fractional bounding frame lengths. The stop criteria are set at 10% convergence between successive analyses, which means that the calculation results cannot differ by more than 10%. When this criterion was achieved, the results were accepted as correct. The imposed conditions were achieved between analyses 4 and 5, with a difference of only 1%, as shown in Figure 25.

The area of maximum stress was invisible, so the results obtained during the first analysis were superimposed (Figure 26).

The maximum stresses occurred at the junction of the four plates and were of a point nature. In addition, this place has been filled with weld, so the actual average stresses will be at a much lower, acceptable level.

Rationality analysis

A rationality analysis was carried out for the presented project. It covered the most important aspects related to the investment, which include: Project objective, Project scope, Cost-benefit analysis, Risk analysis.

Objective of the project

The goal included two aspects – financial, for the client who commissioned the project, and the goal set by the company implementing the project, i.e. to promote hydropower in Poland, where there is no potential to build large hydroelectric power plants. Currently, there is a great need to implement this type of solutions. The obvious

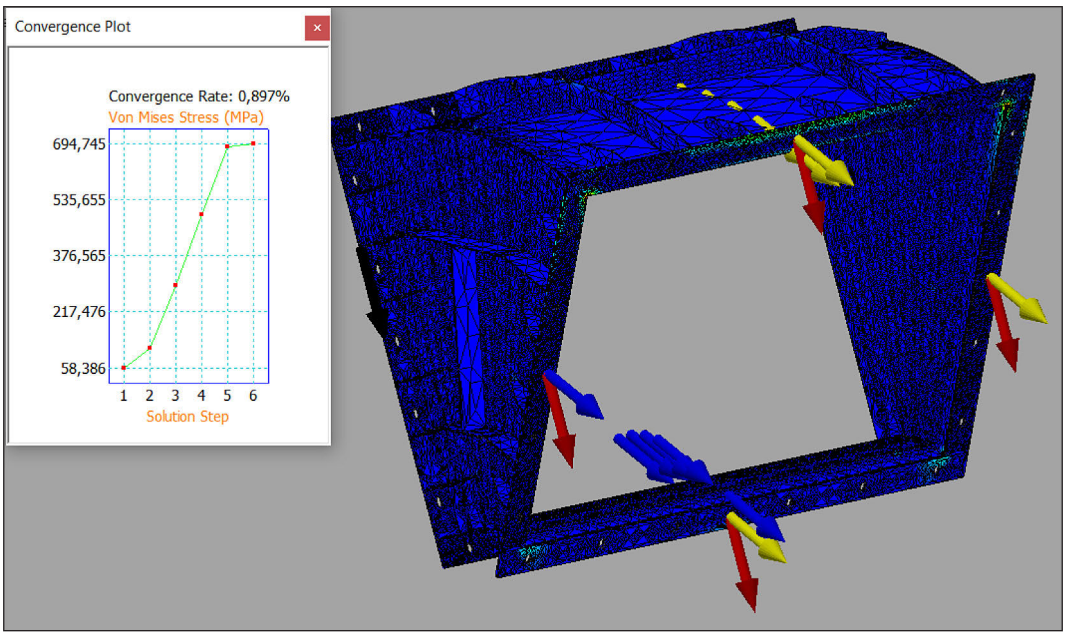

Figure 25. Detailed results of Von Mises Stress analysis

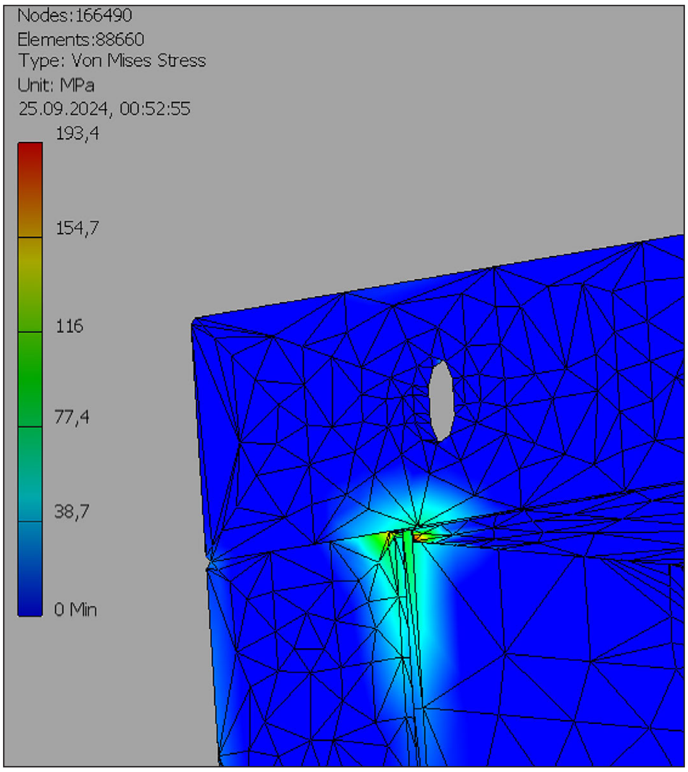

Figure 26. Location of the greatest Von Mises stress

purpose of building installations that obtain electricity from watercourses is to increase the amount of energy obtained from renewable sources. This is particularly important in countries such as Poland, where there is no potential for the development of hydropower.

Project scope

The scope included the selection of the location where it would be possible to obtain building permits, and then in order: design execution, installation assembly, commissioning and testing, commissioning and operation monitoring.

The location chosen for the project is a place where another power plant with a different design previously operated. In such a place, it is easier to obtain a building permit, which is further facilitated by the fact that there is a water threshold in this place, which is a remnant of the mill.

The design, assembly, commissioning and testing were supervised by the construction company Prorys. The construction part was completed in December 2020. The execution and installation were completed in June 2021. After the start-ups, a decision was made to modify the power plant and expand it with a gearbox. This solution also allowed for the use of a commercial generator, which allowed for rational use of the power generated by the rotor. At the beginning of December 2021, the unit was modified and put into operation.

Monitoring of the power plant provided information on the average water flow through the turbine, which amounted to 2.4 m^3/s, and the level of annual average production, which amounted to 150 MWh (megawatt hours). The above parameters were achieved with a water accumulation of 1.9 m of liquid column.

Cost-benefit analysis

The cost of the construction part was less than 100 thousand PLN. The modernization of the river course, automation and electrical connections slightly exceeded the value of 100 thousand PLN. The whole cost the investor over 200 thousand PLN (this information was obtained). The investor also shared information that the monthly profit from the power plant is 5–6 thousand PLN, which means that the entire investment will pay for itself in 4–5 years of continuous operation, and then it will generate profits.

The benefits of power plants are, of course, financial benefits for the investor, but also an increase in the share of renewable electricity sources in the energy sector, which is a huge benefit for society. In addition, such energy is cheap and clean (no pollutant emissions occur during processing), and as it is classified as a renewable source, it increases energy security and ensures the stability of energy supply to places with limited access to other sources.

Risk analysis

The problems that arose in connection with the construction of the power plant were primarily the difficulties caused by the need to build a dam. At high water level, free flow is restricted. The construction and operation of the power plant required the damming of water, which has certain consequences not only for the surrounding flora and fauna, but also for people who have summer houses nearby. The surrounding areas have been flooded, which is particularly noticeable when the water level in the river rises.

The threat posed by the power plant to fish and birds was eliminated at the design stage by using WEMA screens.

CONCLUSIONS

Numerical calculations were carried out and the results were presented, focusing on three main areas: Von Mises stresses, displacements and the factor of safety. The results obtained in all three areas were in line with the assumptions and did not exceed the permissible values, which proves that the solutions were properly selected at the stage of designing the power plant and that there was no need to make any structural changes. The most loaded segment of the installation, which was selected by means of analytical calculations, i.e. the segment that is the weakest link, due to the fact that it is more (or even much more) loaded than the others, was subjected to numerical analysis.

REFERENCES

1. Tondini F., Basso A., Arinbjarnar U., Nielsen C.V. The Performance of 3D printed polymer tools in sheet metal forming, Advances in Metals 2021; 11(8).
2. Bradac J., Sobotka J. Influence of draw-beads geometry on the surface quality of zn-mg coating, Advances in Manufacturing Technology 2021; 13(6): 758–768.
3. https://autokult.pl/materialy-konstrukcyjne-w-nowoczesnych-pojazdach samochodowychcz-1,6808815326357121a [23.01.2024r.]
4. Tan H., Liu C., Chen C., Wang J. An intelligent approach to design three-dimensional aircraft sheet metal part model for manufacture. In: Proceedings of the 11th International Conference on Manufacturing Research (ICMR2013), Castellon, Spain 2013, 83–88.
5. MacDonald B.J. A computational and experimental analysis of high Energy impact to sheet metal aircraft structures, Advances in Journal of Materials processing technology 2002; 124: 92–98.
6. Niezgoda T., Małachowski J., Budzyński A., Kościanowski S. Model 3D MCAD lekkiego samolotu sportowego, jako źródło geometrii dla analizy wytrzymałościowej MES obiektu. In: IX Krajowa Konferencja Naukowo-Techniczna: Programy MES w Komputerowym Wspomaganiu Projektowania i Wytwarzania, Giżycko, Poland 2005.
7. Wang S., Dai J., Wang J., Li R., Wang J., Xu Z. Numerical Calculation of High-Strength-Steel Saddle Plate Forming Suitable for Lightweight Construction of Ships. Advances in Materials 2023; 16(10).
8. Hwang S.Y., Lee J.H., Yang Y.S., Yoo M.J. Springback adjustment for multi-point forming of thick plates in shipbuilding. Advances in Computer-Aided Design 2010; 42(11): 1001–1012.
9. Abedini, S., Schäfer, S., Bäcker, F., Ludwig, C. Geometric figures and potential component families of metal sheets for the use in architecture. In Building Skins Conference, Graz, Austria 2012.
10. Seitzberger, M., Nedelik, R., Ruthmeier, A., Grausgruber, T. CAE-based concept development for lightweight design of railway vehicles. Advances in: Lightweight Design worldwide 2017; 10: 32–37.
11. Gujarathi, M.P., Patil, M.O., Mhatre, M.T., Bokde, M.P. Automatic pneumatic sheet metal feeding and cutting machine. Advances in IJraset 2021; 9(11): 150–165.
12. Carbogno, A., Stawowiak, M., Jasiński, T. Problematyka górniczego wyciągu szybowego szybu 2.1 zakładu górniczego LW” Bogdanka” SA. Advances in: Napędy i Sterowanie 2018; 20: 44–55.
13. Michałek M. Koncepcja rozwiązań konstrukcyjnych zabezpieczenia wyrobisk podszybia adaptowanego na potrzeby podziemnego zbiornika. Advances in: Górnictwo i Geoinżynieria 2007; 3(1): 429–438.
14. Andrejiová, M., Grinčová, A. The experimental research of the conveyor belts damage used in mining industry. Advances in Acta Montanistica Slovaca 2016; 21(3): 180–190.
15. 15. Awuah-Offei, K., Checkel, D., Askari-Nasab, H. Evaluation of belt conveyor and truck haulage systems in an open pit mine using life cycle assessment. Advances in CIM Magazine 2009; 4(5).
16. Demir, N., Sucuoğlu, H. S., Böğrekci, İ., Demircioğlu, P. Structural & dynamic analyses and simulation of mobile transportation robot. Advances

in International Journal of 3D Printing Technologies and Digital Industry 2021; 5(3): 587–595.

17. Coetzee, S., Swart, H., Bosscha, P., Oosthuizen, D. Design of an industrial all-terrain robot platform lessons learned in the design of a robotic mine safety platform for South African gold mines. In 5th Robotics and Mechatronics Conference of South Africa, Johannesberg, South Africa 2012: 1–4.
18. Hingu, P.R., Panchal, D.N. Industrial robot and automation. Advances in The International Journal of Engineering and Science (IJES) 2021; 10(2): 15–23.
19. Prabhakaran, S., Aravinth Kumar, T., Adhik Namo, V. Design and analysis of autonomous mobile robot. Advances in Nveo-Natural Volatiles & Essential Oils Journal| NVEO 2021; 8: 3020–3030.
20. Krishnamoorthy, K. Design and development of a lead screw gripper for robotic application. Advances in Mechatronics and Applications: An International Journal (MECHATROJ) 2019; 2(1)
21. Ślipek, Z., Frączek, J., Cieślikowski, B. Specyfikacja ogólnych wymagań projektowych dla maszyn rolniczych. Cz. II. Maszyny do zbioru. Advances in Inżynieria Rolnicza 2008; 12: 291–298.
22. Ishibashi, T. Hironaka S. Araki N. Development of high reliability rolling bearings and drive shafts for agricultural and construction machinery. Advances in JTEKT Engineering Journal 2015; 1012E: 62–69.
23. Gwizdal P., Gola A., Święć A. Projekt i wdrożenie elektrowni wodnej lewarowej na rzece Bystrzyca w Lublinie, Advances in Polskie Wydawnictwo Ekonomiczne 2022: 141–149.